Syntheses, Structures, and Properties of a Series of Metal Ion-Containing Dialkylimidazolium Ionic Liquids

Chongmin Zhong,[1] Takehiko Sasaki,*[2] Akiko Jimbo-Kobayashi,[3] Emiko Fujiwara,[3] Akiko Kobayashi,[3,4] Mizuki Tada,[1] and Yasuhiro Iwasawa[1]

[1]Department of Chemistry, Graduate School of Science, The University of Tokyo, Hongo, Bunkyo-ku, Tokyo 113-0033

[2]Department of Complexity Science and Engineering, Graduate School of Frontier Sciences, The University of Tokyo, 5-1-5 Kashiwanoha, Kashiwa 277-8561

[3]Research Center for Spectrochemistry, Graduate School of Science, The University of Tokyo, Hongo, Bunkyo-ku, Tokyo 113-0033

[4]Department of Chemistry, College of Humanities and Sciences, Nihon University, 3-25-40 Sakurajosui, Setagaya-ku, Tokyo 156-8550

Received June 25, 2007; E-mail: takehiko@k.u-tokyo.ac.jp

A series of metal ion-containing ionic liquids [Bmim]$_2$[MCl$_4$] (M = Sn, Cu, Ni, Mn, Fe, Co, Zn, and Pt; [Bmim] = 1-butyl-3-methylimidazolium) and [Bmim]$_2$[ZrCl$_6$] were synthesized and their single-crystal structures were determined by X-ray crystallographic analysis. The crystal structures showed the existence of an interaction between chlorometalate anions and imidazolium cations via C–H⋯Cl hydrogen bonding as well as an interaction between the cations through C–H⋯π hydrogen bonding and/or π⋯π stack interaction. The melting points of the metal salts were found to correlate with the number of halide ions coordinated to each metal ion and the overall symmetry of the chlorometalate anions. Ionic conductivity measured in super-cooled states of the synthesized salts unambiguously confirmed that these salts behaved as ionic liquids. The synthesized salts have a high thermal stability as evaluated by TGA and negligible vapor pressure before decomposition.

Ionic liquids have received much attention because of their versatile applications[1–7] such as electrolytes in electrochemistry, environmentally friendly solvents in organic synthesis, and immobilizing phases for biphasic catalysis. They are also regarded as precursor materials for catalysts.[8–10] Dialkylimidazolium and *N*-alkylpyridinium or quaternary ammonium-based salts are typical ionic liquids most widely studied due to the ease of synthesis. The completely ionic nature of ionic liquids makes them useful as solvents for highly charged complexes, and the low vapor pressure of ionic liquids makes it possible to use them in vacuum and as "green" solvents in industrial processes.[11]

Since metal ion-containing ionic liquids find various applications in catalysis and other technologies, determination of their structures and measurements of their physical and chemical properties are important. Scheffler and Thomson have reported the preparation of ionic liquids by mixing a variety of metal chlorides (AgCl, CuCl, LiCl, CdCl$_2$, CuCl$_2$, SnCl$_2$, ZnCl$_2$, LaCl$_3$, YCl$_3$, SnCl$_4$, and TiCl$_4$) with [Emim]Cl (Emim = 1-ethyl-3-methylimidazolium).[12] Abbott et al. have prepared ionic liquids based on metal halides (Zn, Fe, and Sn) and substituted quaternary ammonium salts, for which they have measured freezing points, viscosity, electrochemical potentials, and FAB mass spectra.[13,14] Brown et al. have prepared [Bmim][Co(CO)$_4$] (Bmim = 1-butyl-3-methylimidazolium) and showed its catalytic activity for the debromination of 2-bromoketones.[15] Crystal structures of [Emim]$_2$[VOCl$_4$],[16]

[Emim]$_2$[CoCl$_4$],[17] [Emim]$_2$[NiCl$_4$],[17] [Bmim]$_2$[PdCl$_4$],[8] [Emim][AuCl$_4$],[18] [Bmim][AuCl$_6$],[18] [Emim]$_2$[PtCl$_6$],[19] [Emim]$_2$[PtCl$_4$],[19] [Emim]$_2$[IrCl$_6$],[19] and [Bmim]Cl[20,21] have been reported. Previous crystallographic studies have shown that, in imidazolium-based ionic liquids, the ring protons of imidazolium cation can form hydrogen bonds with chlorine atoms of the chlorometalates[17,22,23] and nitrogen atom of [Ag(CN)$_2$]$^-$ anion.[24]

It is still unclear whether such metal-containing salts behave as ionic liquids or not. Measurement of ionic conductivity as a function of temperature[25–27] is a straightforward method to prove that a sample is comprised of ions in the liquid phase and the ionic conductivities of metal salts, such as [Emim][NbF$_6$],[28] [Emim][TaF$_6$],[28] [Emim][FeCl$_3$],[29] [Emim][FeCl$_4$],[29] and [Bmim][FeCl$_4$][30] have been measured. Physical properties like magnetic property, viscosity, and density of salts involving transition-metal chlorides have also been reported.[31,32] UV, Raman spectroscopy, and Superconducting Quantum Interface Device (SQUID) measurements of [Bmim]Cl/FeCl$_2$ or FeCl$_3$[33,34] have also been examined. Thus, physical and chemical properties of metal ion-containing salts have been investigated from fundamental interests of themselves and practical viewpoints for a variety of applications.

The aim of the present study was to synthesize a series of metal ion-containing ionic liquids and to determine their structures. In addition, their physical properties, such as ionic conductivity and thermal properties, were examined, because of

their versatile application to catalysts and ionic conductive materials. Cu- and Ni-containing ionic liquids among the synthesized ones have been found to be active for catalytic organic reactions.[10,35] The ionic conductivity and thermal property are discussed in relation to the crystal structure and the symmetry of metal chloride anions.

Experimental

Materials. $MnCl_2$ (99+%) and $ZrCl_4$ (99.9%) were obtained from Aldrich. $CoCl_2$ (97.0%), $ZnCl_2$ (99.9%), $NiCl_2$ (99.9%), $PtCl_2$ (98.0%), $FeCl_2$ (98%), $CuCl_2$ (99.99%), and $SnCl_2$ (99.9%) were purchased from WAKO. All of the metal salts were anhydrous. Anhydrous redistilled 1-methylimidazole (99+%) was purchased from Aldrich. 1-Chlorobutane (98.0%) and all of the dehydrated solvents (H_2O <50 ppm) were purchased from WAKO. All chemicals were used without further purification.

General Techniques. ^1H and ^{13}C NMR spectra in CD_3CN were recorded on a Bruker DRX-500 spectrometer using TMS as an internal standard. The peak assignments in ^1H and ^{13}C NMR spectra of [Bmim]Cl and [Bmim]$_2$[NiCl$_4$] were made according to the results of COSY, HMQC, and HMBC. Assignments of the ^1H and ^{13}C NMR spectra of the other compounds were made by comparing with the results of [Bmim]Cl and [Bmim]$_2$[NiCl$_4$]. Elemental analysis was performed at the Analytical Laboratory of the Department of Chemistry, Faculty of Science, the University of Tokyo using a Yanaco CHNCORDER MT6 automatic elemental analyzer. TGA (Thermogravimetric Analysis) was recorded on a Rigaku TG-8120 instrument in an Al pan using Al_2O_3 as standard. Samples (10 mg) were heated from 298 to 673 K at a ramping rate of 10 K min^{-1} under nitrogen atmosphere. Melting points were measured by observing each crystal fused in a capillary under nitrogen upon elevating temperature. Melting points measured in this way agreed with the position of DTA peaks obtained in the TGA measurements. The vapor pressures of ionic liquids were measured using a capacitance diaphragm gauge (Varian CDG GAUGE, range 0–1000 Torr). Into a glass tube, the sample (0.0818 mmol) was added, and the tube was connected to the gauge and the system was evacuated over 30 min. The system was closed and heated from 293 to 873 K at 10 K min^{-1}. The ionic conductivity was measured using an electrical meter CM-60G (DKK TOA corporation G-series). Glass conductivity cell with two platinum electrodes was used, and the cell constant was 102.1 m^{-1}. This electrometer uses an AC impedance method with a frequency of 80 Hz below 20 mS m^{-1} and 3 kHz above 20 mS m^{-1}. Calibration of the instrument was carried out with a 0.1 mol L^{-1} KCl solution. Ionic conductivity measurements were performed on our home-made apparatus under dry nitrogen. The conductivity cell (15-mm glass tube) was fitted into the apparatus with a viton O-ring so that evacuation and dry nitrogen supply were possible for these measurements. Each sample was evacuated for 24 h before the measurement.

Syntheses.   The synthetic route for the ionic liquids is shown in Scheme 1. A mixture of 1-methylimidazole and *n*-butyl chloride was degassed by freeze–pump–thaw cycles three times and then filled with nitrogen. The reaction between 1-methylimidazole and *n*-butyl chloride resulted in the salt [Bmim]Cl (**1**). Salt **1** was purified by recrystallization from acetonitrile solution at 263 K to remove the yellow color of the initial crude product. It should be noted that the addition of a little crystal seeds is necessary to start crystallization. In the next step, **1** was reacted with metal chlorides $SnCl_2$ and $CuCl_2$ without solvent at 298 and
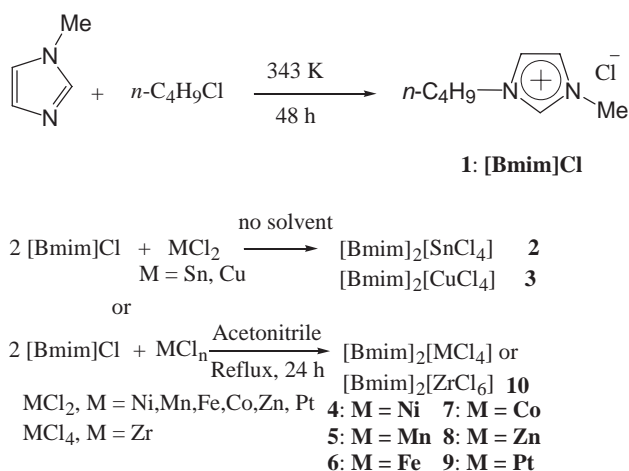
Scheme 1. Synthesis of the metal ion-containing ionic liquids.

373 K, or $NiCl_2$, $MnCl_2$, $FeCl_2$, $CoCl_2$, $ZnCl_2$, $PtCl_2$, and $ZrCl_4$ in acetonitrile at 363 K, which afforded nine metal-containing salts [Bmim]$_2$[SnCl$_4$] (**2**), [Bmim]$_2$[CuCl$_4$] (**3**), [Bmim]$_2$[NiCl$_4$] (**4**), [Bmim]$_2$[MnCl$_4$] (**5**), [Bmim]$_2$[FeCl$_4$] (**6**), [Bmim]$_2$[CoCl$_4$] (**7**), [Bmim]$_2$[ZnCl$_4$] (**8**), [Bmim]$_2$[PtCl$_4$] (**9**), and [Bmim]$_2$[ZrCl$_6$] (**10**), respectively. Salts **2** and **3** are liquids, and the others are solids at room temperature. All of the salts, except **2** and **3**, were recrystallized from acetonitrile solution at an appropriate temperature. Crystals of [Bmim]$_2$[CuCl$_4$] (**3**) and [Bmim]$_2$[SnCl$_4$] (**2**) were grown in dry acetonitrile solution at 223 K and acetonitrile/diethyl ether at 245 K, respectively. **2** was crystallized by freezing its acetonitrile solution with liquid nitrogen, and adding diethyl ether onto the formed solid and keeping the solid–liquid mixture in refrigerator at 245 K for several days. In order to start the crystallizing process and to obtain crystals with a good shape, the addition of small crystal seeds to solution is indispensable. A small amount of crystals of **2** was obtained by painting a layer of the salt on the glass wall of a Schlenk tube and keeping the tube at 245 K for about one month.

The compositions of salts **1**–**10** were determined by using elemental analysis and ^1H and ^{13}C NMR. Assignments of NMR spectra are described in the Supporting Information. The chemical shifts of NC*H*N on imidazolium rings appeared at 8.7–9.5 ppm except for salts **4** and **5**, for which the chemical shifts moved to 4.44 ppm for **4**, and 3.85 ppm for **5**. These results indicate that the ring hydrogen of NC*H*N in **4** and **5** has a specific interaction with [MCl$_4$] anion in solution phase.

Purity of a sample was estimated based on results of elemental analyses. Water was regarded as the main impurity judging from the deviation in elemental analyses. The water content (wt %) of each sample was calculated from the averaged deviation between the calculated and the observed values (C, H, and N) in elemental analyses: BmimCl (**1**), 4.6%; [Bmim]$_2$[SnCl$_4$] (**2**), 4.2%; [Bmim]$_2$-[CuCl$_4$] (**3**) 0.4%; [Bmim]$_2$[NiCl$_4$] (**4**), 1.9%; [Bmim]$_2$[MnCl$_4$] (**5**) 1.2%; [Bmim]$_2$[FeCl$_4$] (**6**), 1.0%; [Bmim]$_2$[CoCl$_4$] (**7**), 0.8%; [Bmim]$_2$[ZnCl$_4$] (**8**), 0.7%; [Bmim]$_2$[PtCl$_4$] (**9**), 5.5%; [Bmim]$_2$-[ZrCl$_6$] (**10**), 1.3%.

Crystal Structure Analyses.   Single crystals of synthesized salts were sealed in capillary tubes under nitrogen for X-ray structure analysis. X-ray crystallographic data for all of the crystals were collected on a Rigaku/MSC Mercury CCD system with graphite monochromated Mo Kα radiation ($\lambda = 0.71070$ Å). The collected data were processed by using the Crystal Clear program
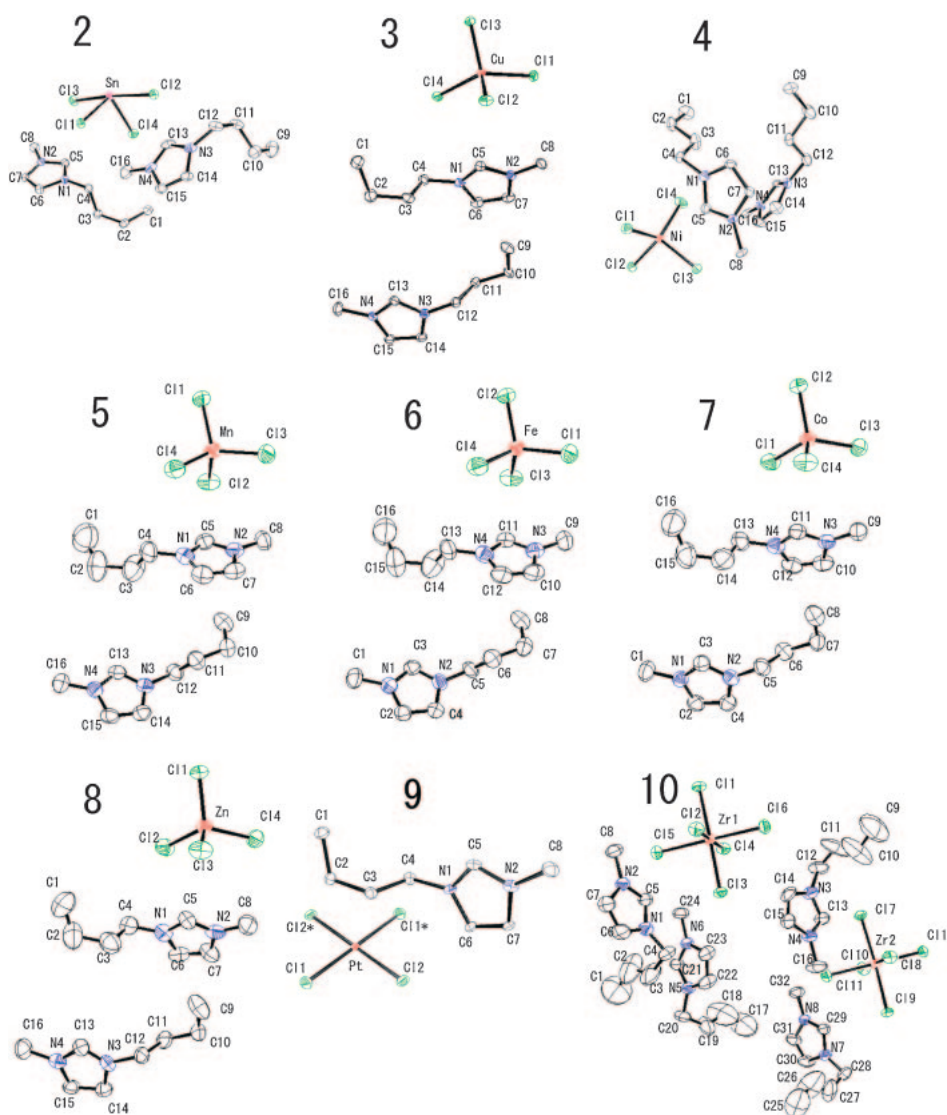
Fig. 1.   ORTEP drawings of [Bmim]$_2$[SnCl$_4$] (**2**), [Bmim]$_2$[CuCl$_4$] (**3**), [Bmim]$_2$[NiCl$_4$] (**4**), [Bmim]$_2$[MnCl$_4$] (**5**), [Bmim]$_2$[FeCl$_4$] (**6**), [Bmim]$_2$[CoCl$_4$] (**7**), [Bmim]$_2$[ZnCl$_4$] (**8**), [Bmim]$_2$[PtCl$_4$] (**9**), and [Bmim]$_2$[ZrCl$_6$] (**10**) at 50% probability except **10** which is at 30% probability. Hydrogen atoms are omitted for clarity.

(Rigaku). The structures were solved by direct methods (SIR92),[36] expanded using Fourier techniques and refined with full-matrix least-squares method using the refinement program package Texan (Rigaku). The non-hydrogen atoms were refined anisotropically for all the structures. Positions of hydrogen atoms were calculated and included in the analysis. Absorption correction by using an empirical method was adopted for all structures.

Crystallographic data have been deposited with Cambridge Crystallographic Data Centre: Deposition number CCDC-639882–639890 for compound Nos. 2–10. Copies of the data can be obtained free of charge via http://www.ccdc.cam.ac.uk/conts/retreiveing.html (or from the Cambridge Crystallographic Data Centre, 12, Union Road, Cambridge, CB2 1EZ, UK; Fax: +44 1223 336033; e-mail: deposit@ccdc.cam.ac.uk).
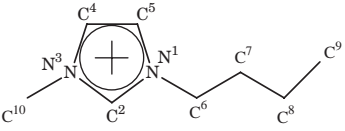
Results and Discussion

Crystal Structures.   Determination of the single crystal structures of [Bmim]$_2$[MCl$_4$] (M = Sn (**2**), Cu (**3**), Ni (**4**), Mn (**5**), Fe (**6**), Co (**7**), Zn (**8**), and Pt (**9**)) and [Bmim]$_2$[ZrCl$_6$]

(**10**) was performed, and ORTEP drawings[37] for the asymmetric units of **2**–**10** are depicted in Fig. 1. The experimental details and crystallographic data for the salts **2**–**10** are presented in Table 1. XRD measurements were performed at 203 K for **2**, 113 K for **3**, **4**, and **9**, and at 298 K for the other salts. All nine salts belonged to a monoclinic system, but they showed different crystallographic space groups: $P2_1/a$ for **2**, Cc for **3**–**8**, $P2_1/n$ for **9**, and $P2_1$ for **10**. For each salt assigned as being in the space group Cc, the presence of inversion symmetry was examined, and analysis based on the space group $C2/c$ was peformed, which supported the assignment of Cc as the space group. Similarly, for the Zr salt assigned as being in the space group $P2_1$, the presence of inversion symmetry was examined, and analysis based on the space group $P2_1/m$ confirmed the assignment of $P2_1$ as the space group. The asymmetric units, i.e., the crystallographically independent molecules of **2**–**8**, involve two cations and one anion: that of **10** contains four cations and two anions; and that of **9** contains only one cation and half anion. The two imidazolium rings in **3**

Table 1. Experimental Conditions and Crystallographic Data for [Bmim]$_2$[SnCl$_4$] (**2**), [Bmim]$_2$[CuCl$_4$] (**3**), [Bmim]$_2$[NiCl$_4$] (**4**), [Bmim]$_2$[MnCl$_4$] (**5**), [Bmim]$_2$[FeCl$_4$] (**6**), [Bmim]$_2$[CoCl$_4$] (**7**), [Bmim]$_2$[ZnCl$_4$] (**8**), [Bmim]$_2$[PtCl$_4$] (**9**), and [Bmim]$_2$[ZrCl$_6$] (**10**)

	2	**3**	**4**	**5**	**6**	**7**	**8**	**9**	**10**
Formula	C$_{16}$H$_{30}$Cl$_4$SnN$_4$	C$_{16}$H$_{30}$Cl$_4$CuN$_4$	C$_{16}$H$_{30}$Cl$_4$NiN$_4$	C$_{16}$H$_{30}$Cl$_4$MnN$_4$	C$_{16}$H$_{30}$Cl$_4$FeN$_4$	C$_{16}$H$_{30}$Cl$_4$CoN$_4$	C$_{16}$H$_{30}$Cl$_4$ZnN$_4$	C$_{16}$H$_{30}$Cl$_4$PtN$_4$	C$_{16}$H$_{30}$Cl$_6$ZrN$_4$
FW	538.94	483.80	478.95	475.19	476.10	479.18	485.63	615.34	582.38
Crystal color	Colorless	Yellow	Blue	Yellowish green	Light purple	Blue	Colorless	Red	Colorless
Crystal system	monoclinic	monoclinic	monoclinic	monoclinic	monoclinic	monoclinic	monoclinic	monoclinic	monoclinic
Space group	$P2_1/a$	Cc	Cc	Cc	Cc	Cc	Cc	$P2_1/n$	$P2_1$
a/Å	14.074(2)	14.090(2)	9.450(1)	14.669(4)	14.583(2)	14.582(2)	14.573(2)	8.684(2)	8.806(1)
b/Å	9.648(1)	9.719(1)	16.410(1)	9.835(2)	9.8316(9)	9.808(1)	9.8169(8)	10.644(3)	17.730(2)
c/Å	17.917(3)	17.167(3)	15.439(2)	17.248(4)	17.199(2)	17.107(3)	17.091(2)	11.745(3)	17.751(2)
β/deg	108.156(2)	107.356(3)	104.946(2)	108.345(1)	108.374(2)	108.3952(5)	108.329(2)	90.9882(9)	90.0212(7)
V/Å^3	2311.9(6)	2243.8(6)	2313.3(4)	2361.8(10)	2340.2(5)	2321.5(6)	2321.1(5)	1085.5(3)	2771.6(6)
Z	4	4	4	4	4	4	4	2	4
D_{calcd}/g cm^{-3}	1.548	1.432	1.375	1.336	1.351	1.371	1.390	1.882	1.396
F_{000}	1088.00	1004.00	1000.00	988.00	992.00	996.00	1008.00	600.00	1184.00
μ(Mo Kα)/cm^{-1}	15.74	14.56	13.07	10.18	11.07	12.06	15.25	69.37	9.83
Temp/K	203	113	113	298	298	298	298	113	298
Reflections measured	18363	9023	9343	9464	9501	9239	9295	8668	22198
Unique reflections	4600	2481	2233	2373	2005	2367	2380	2118	5315
No. of reflections	4080 ($I > 3\sigma(I)$)	2337 ($I > 3\sigma(I)$)	1671 ($I > \sigma(I)$)	1736 ($I > 3\sigma(I)$)	956 ($I > 3\sigma(I)$)	2164 ($I > 3\sigma(I)$)	1674 ($I > 2\sigma(I)$)	1666 ($I > 3\sigma(I)$)	4563 ($I > 3\sigma(I)$)
No. of variables	226	227	227	227	127	227	227	115	488
$R1$[a]	0.032 ($I > 3\sigma(I)$)	0.033 ($I > 3\sigma(I)$)	0.042 ($I > \sigma(I)$)	0.039 ($I > 3\sigma(I)$)	0.061 ($I > 3\sigma(I)$)	0.039 ($I > 3\sigma(I)$)	0.045 ($I > 2\sigma(I)$)	0.023 ($I > 3\sigma(I)$)	0.032 ($I > 3\sigma(I)$)
R_w[b]	0.150	0.092	0.131	0.097	0.221	0.115	0.148	0.064	0.076
GOF	2.33	1.43	0.84	0.96	2.92	1.70	0.90	0.55	0.85

a) $R1 = \Sigma||F_o| - |F_c||/\Sigma|F_o|$. b) $R_w = [\Sigma w(F_o^2 - F_c^2)^2/\Sigma w(F_o^2)^2]^{1/2}$, where the least-squares weights were estimated by the formula: $w = 1/\sigma^2(F_o^2)$.

C. Zhong et al.

Bull. Chem. Soc. Jpn. Vol. 80, No. 12 (2007) 2369

Table 2. Conformations of the Butyl Chains in [Bmim]$_2$-[MCl$_x$][a)]

Entry	ILs	Conformation	
		C^6–C^7	C^7–C^8
1	[Bmim]$_2$[SnCl$_4$][b)]	gauche	anti
		anti	gauche
2	[Bmim]$_2$[CuCl$_4$]	anti	gauche
3	[Bmim]$_2$[NiCl$_4$]	anti	anti
4	[Bmim]$_2$[MnCl$_4$]	anti	gauche
5	[Bmim]$_2$[FeCl$_4$]	anti	gauche
6	[Bmim]$_2$[CoCl$_4$]	anti	gauche
7	[Bmim]$_2$[ZnCl$_4$]	anti	gauche
8	[Bmim]$_2$[PtCl$_4$]	anti	gauche
9	[Bmim]$_2$[ZrCl$_6$]	gauche	anti

a) Atom numbering nomenclature for [Bmim] cation. Hydrogen atoms are denoted with the number associated with the carbon atoms, for example, hydrogen atom bonding with C^2 is denoted as H^2. b) Two cations are contained in the asymmetric unit of [Bmim]$_2$[SnCl$_4$], having gauche/anti and anti/gauche conformations.

are nearly parallel to each other and the two butyl chains are directed to opposite directions. In contrast, the two butyl chains in **4** are nearly perpendicular to each other.

For convenience, two labeling systems are used to refer to the position of the atoms: atom labels derived from the systematic ring numbering nomenclature of the cation, (e.g. N^1, C^2, etc.; see the chart in Table 2) and those from crystallographic labels in the form C1, C2, N1, etc. (see Fig. 1).

The local structures around anions in [Bmim]$_2$[MCl$_4$] (M = Sn (**2**), Cu (**3**), and Ni (**4**)), [Bmim]$_2$[PtCl$_4$] (**9**), and [Bmim]$_2$[ZrCl$_6$] (**10**) are illustrated in Fig. 2, where the dotted lines show the hydrogen bonds between H and chloride ions shorter than 2.95 Å, which is the sum of the van der Waals radii of H and Cl atoms. It is noted that all of the chlorine atoms except one in **4** are involved in a complex three-dimensional hydrogen-bonding network. The hydrogen atoms that can form strong hydrogen bonds with chlorine atoms are those of imidazolium ring (C^2, C^4, and C^5) and α-carbon of the butyl group (C^6). The hydrogen atoms of methyl group cannot form strong hydrogen bond in all these nine salts. All Bmim cations have planar 5-membered imidazolium rings, and the conformation of butyl groups was found to depend on the anions, which will be mentioned later.

The averaged M–Cl bond lengths in [Bmim]$_2$[MCl$_4$] (M = Cu (**3**), Ni (**4**), Mn (**5**), Fe (**6**), Co (**7**), and Zn (**8**)) are 2.254 Å for **3**, 2.249 Å for **4**, 2.360 Å for **5**, 2.311 Å for **6**, 2.274 Å for **7**, and 2.267 Å for **8**. The anions in **5**–**8** are situated in an approximately tetrahedral T_d symmetry. Because of Jahn–Teller effect,[38] the anion [CuCl$_4$]$^{2-}$ exhibits a distorted tetrahedral geometry with approximately D_{2d} symmetry, and the average Cl–Cu–Cl angle is 127.2°. A survey of 62 crystal structures containing discrete [CuCl$_4$]$^{2-}$ ions[39,40] indicated that the mean Cl–Cu–Cl angle ranges from 105.2° in C$_{42}$H$_{44}$-
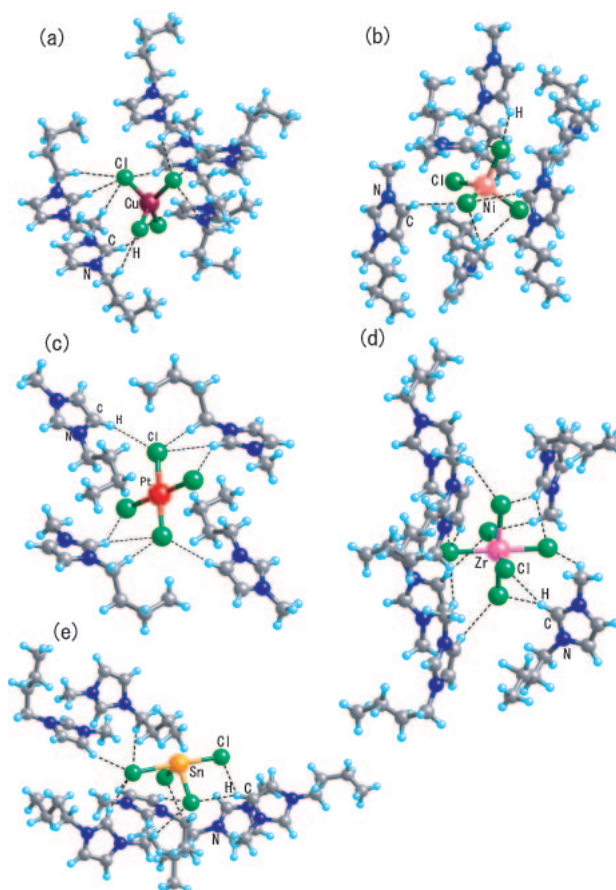

Fig. 2. Local structure around an anion for (a) [Bmim]$_2$-[CuCl$_4$] (**3**), (b) [Bmim]$_2$[NiCl$_4$] (**4**), (c) [Bmim]$_2$[PtCl$_4$] (**9**), (d) [Bmim]$_2$[ZrCl$_6$] (**10**), and (e) [Bmim]$_2$[SnCl$_4$] (**2**). The dotted lines show the hydrogen bonds between H and Cl shorter than 2.95 Å.

O$_2$P$_2$CuCl$_4$ to 180.0° in (PhCH$_2$CH$_2$NMeH$_2$)$_2$[CuCl$_4$]. The [NiCl$_4$]$^{2-}$ anion has a distorted tetrahedral geometry, and the mean angle of Cl1–Ni–Cl3 and Cl1–Ni–Cl4 is 115.8°. The [PtCl$_4$]$^{2-}$ anion in **9** and the [ZrCl$_6$]$^{2-}$ anion in **10** have a square-planar geometry and an octahedral geometry, respectively. The [SnCl$_4$]$^{2-}$ anion in **2** (Fig. 1) exhibits a pseudotrigonal bipyramidal geometry with approximately C_{2v} symmetry. It is known that an Sn^{II} cation and chlorine anions form trigonal [SnCl$_3$]$^-$ and pseudotrigonal bipyramidal [SnCl$_4$]$^{2-}$.[41] In trigonal [SnCl$_3$]$^-$, the Cl–Sn–Cl angles are close to 90°, and the Sn–Cl distances have been determined to be between 2.42 and 2.49 Å.[42,43] The pseudotrigonal bipyramidal [SnCl$_4$]$^{2-}$ has also been reported to exist in [Co(NH$_3$)$_3$][SnCl$_4$]Cl,[43] in which the Sn–Cl distances are 2.526 and 2.467 Å for equatorial bonds, and 3.003 and 2.669 Å for axial bonds; the Cl–Sn–Cl angles are 89.98° (equatorial) and 164.69° (axial). The equatorial Sn–Cl distances in **2** are 2.502 and 2.487 Å. The distances of the two axial bonds are definitely different: 2.682 Å for the shorter one and 2.866 Å for the longer one. The bond angles of Cl–Sn–Cl are 95.21° in the equatorial direction and 176.07° in the axial direction.

Hydrogen Bonding and Weak Interactions in Crystals. Hydrogen bonds play important roles in molecular recognition processes[44–46] and crystal engineering.[47] The presence of weak

Table 3. Symmetry of Anions, Melting Points, and Decomposition Temperatures for Ionic Liquids

Entry	Ionic liquids[a)]	Symmetry of anions	Mp/K	Decomp. Temp/K[b)]	Ref.
1	[Bmim]Cl		341	477	This work
2	[Bmim]$_2$[SnCl$_4$]	C_{2v}(distorted)	278	507	This work
3	[Bmim]$_2$[CuCl$_4$]	D_{2d}	296	461	This work
4	[Bmim]$_2$[NiCl$_4$]	T_d(distorted)	329	542	This work
5	[Bmim]$_2$[MnCl$_4$]	T_d	336	566	This work
6	[Bmim]$_2$[FeCl$_4$]	T_d	331	550	This work
7	[Bmim]$_2$[CoCl$_4$]	T_d	335	566	This work
8	[Bmim]$_2$[ZnCl$_4$]	T_d	333	562	This work
9	[Bmim]$_2$[PtCl$_4$]	D_{4h}	372	450	This work
10	[Bmim]$_2$[ZrCl$_6$]	O_h	391	561	This work
11	[Emim]Cl		357		[22]
12	[Emim]Br		354		[22]
13	[Emim]I		354		[22]
14	[Emim][NbF$_6$]	O_h	545		[28]
15	[Emim][TaF$_6$]	O_h	548		[28]
16	[Emim]$_2$[CoCl$_4$]	T_d	374		[17]
17	[Emim]$_2$[NiCl$_4$]	T_d	365		[17]
18	[Emim]$_2$[PtCl$_4$]	D_{4h}	501		[19]
19	[Dmim]CH$_3$SO$_3$	D_{2h}	316		[60]
20	[Dmim]PF$_6$	O_h	362		[61]

a)   [Bmim] = 1-butyl-3-methylimidazolium,   [Emim] = 1-ethyl-3-methylimidazolium, [Dmim] = 1,3-dimethylimidazolium. b) Decomposition temperatures were estimated as temperatures at 1% weight loss in TGA.

hydrogen bonds, C–H⋯Cl, has been established through statistical analysis of published crystal structures in Cambridge Structural Database (CSD).[48,49] The existence for C–H⋯Cl$^-$ hydrogen bonds can be inferred from H⋯Cl$^-$ distance shorter than 2.95 Å together with the C–H⋯Cl$^-$ angle.[50] Another type of hydrogen bond, C–H⋯π geometry, is also very common both in solid state and solution. The C–H group in a C–H⋯π hydrogen bond may interact with the centroid of the aromatic ring or with one or more of the individual ring carbon atoms. Compared with the typical energy of covalent bond (170 kJ mol^{-1}) and van der Waals interaction (1 kJ mol^{-1}),[47] the weak hydrogen bonds mentioned above are about several tens of kilojoules per mole. Despite the relative weakness, their structural effects are surprisingly noticeable in crystal packing.[47] Among the crystal structures in the present study, three types of interactions were found, (1) C–H⋯Cl hydrogen bond, (2) C–H⋯π (imidazolium ring), and (3) π–π stack interaction, as mentioned in detail in the Supporting Information.

Conformation of Butyl Group of Bmim Cation. In all of the structures of the cations in salts **2–10** and reported structures of alkylimidazolium salts available in the CSD database, the β-carbon of the alkyl chain is twisted out of the plane of the imidazolium ring at different angles similar to that found by Holbrey et al.[21] for [Bmim]Cl. The conformation at C^6–C^7 and C^7–C^8 bonds of salts **2–10** are listed in Table 2. Among the four possible combinations of conformation of these bonds, three combinations appeared in Table 2: anti/gauche, gauche/anti, and anti/anti. No gauche/gauche combination was observed because of too large steric strain. The conformation of [Bmim]Cl was analyzed in relation to Raman scattering

bands.[51] [Bmim]Cl is a polymorph of the monoclinic structure and the orthorhombic structure,[21,51] which exhibited anti/anti and gauche/anti conformations, respectively. In liquid phase both anti/anti and gauche/anti conformations were found by Raman scattering.[51] In the present series of salts, in crystal phases, there were various conformations of the butyl group of the Bmim cation, which will be helpful for further vibrational studies.

Melting Point. Melting points of the nine salts were measured, and the results are shown in Table 3 (Entries 1–10) along with the local symmetry of the anions. [Bmim]$_2$[SnCl$_4$] (**2**) melts at 278 K, which is considerably lower than the melting point of a reported SnCl$_2$–butylpyridinium chloride system (mp 295.4 K).[52] [Bmim]$_2$[CuCl$_4$] (**3**) melted at 296 K, which is also considerably low compared to a range of reported organic salts containing discrete [CuCl$_4$]$^{2-}$ anions (e.g., *N*-(2-ammonioethyl)morpholinium tetrachlorocuprate(II), mp 463 K;[53] [(C$_{10}$H$_{21}$)$_2$Cl-im]$_2$[CuCl$_4$]·H$_2$O, mp 403 K).[54] Salts [Bmim]$_2$[MCl$_4$] (M = Ni (**4**), Mn (**5**), Fe (**6**), Co (**7**), and Zn (**8**)) melted at a little higher temperatures around 333 K. These salts could be kept in super-cooled states at room temperature, when the samples once melted were cooled, until they were disturbed by scrubbing the interface between the liquids and vessel. For example, **4** could be kept in a super-cooled state over 30 days. [Bmim]$_2$[PtCl$_4$] (**9**) and [Bmim]$_2$[ZrCl$_6$] (**10**) melted at 372 and 391 K, respectively, and could not be kept in super-cooled states. Stable super-cooled states have been previously reported for various ionic liquid systems.[55–57]

It is known that the melting points of ionic liquids are affected by symmetry of cations,[11] distribution of charge in the

C. Zhong et al.

Bull. Chem. Soc. Jpn. Vol. 80, No. 12 (2007)   2371

cations,[58] size of anions,[59] etc, and Ngo et al.[56] have correlated the melting points of imidazolium-based ionic liquids with the symmetry of imidazolium cations. However, to our knowledge, a correlation between melting point and symmetry of anion has not been made. The melting points of metal salts used in this work are (from low to high): $SnCl_2$, 519 K; $ZnCl_2$, 566 K; $ZrCl_4$, 604 K (sublimation point); $PtCl_2$, 854 K; $CuCl_2$, 893 K; $MnCl_2$, 925 K; $FeCl_2$, 950 K; $CoCl_2$, 997 K; $NiCl_2$, 1274 K. Although the melting point of $ZnCl_2$ is far below those of $CuCl_2$ and $NiCl_2$, the melting point of ionic liquid formed from it (333 K) is well above that of $CuCl_2$ (296 K) and similar to that of $NiCl_2$ (329 K). Because all of these complex salts involve the same [Bmim]$^+$ cation and same molar ratio of cation to anion (2:1), the melting points of ionic liquids are likely to be related to the symmetry of their anions: under the condition of having the same cation, same negatively charged anion, and same molar ratio of cation to anion, ionic liquids with higher symmetry of anions have higher melting points, and the ionic liquids having same symmetry of anions show similar melting points. The degree of symmetry is ordered as follows: $O_h > D_{4h} > T_d > D_{2d} > C_{2v}$. The higher melting points for **9** (372 K) and **10** (391 K) are thought to be caused by the higher symmetry of [PtCl_4]$^{2-}$ and [ZrCl_6]$^{2-}$ (D_{4h} and O_h, respectively). The higher symmetry makes it difficult to keep liquids of these salts in super-cooled states. A higher melting point than that for salt **10** has been reported for [Bmim]$_2$[PtCl_6] (441 K) with the anion having local symmetry O_h.[19] [MCl_4]$^{2-}$ anions (M = Mn, Zn, Co, and Fe) have T_d symmetry and the ionic liquids involving these anions have similar melting points (around 333 K), which are lower than those of **9** and **10**. The distortion of T_d symmetry of [NiCl_4]$^{2-}$ in **4** results in a slight decrease in the melting point of **4** (mp 327 K). [CuCl_4]$^{2-}$ anion has D_{2d} symmetry, which is lower than T_d symmetry, and [Bmim]$_2$[CuCl_4] melts at 296 K. [SnCl_4]$^{2-}$ in **2** (distorted C_{2v}) has the lowest symmetry among the anions of the nine salts, which results in the lowest melting point (278 K). The melting points of other reported ionic liquid salts containing 1-ethyl-3-methylimidazolium ([Emim]) and 1,3-dimethylimidazolium ([Dmim]) cations are also listed in Table 3 for comparison. Emim halide salts (Entries 11, 12, and 13) exhibit remarkably similar melting points ([Emim]Cl, 357 K; [Emim]Br, 354 K; [Emim]I, 354 K).[22] [Emim][NbF_6] (Entry 14) and [Emim][TaF_6] (Entry 15) having anions with the same symmetry (O_h) melt at similar temperatures (545 and 548 K, respectively).[28] For a series of [Emim]$_2$[MCl_4], melting points are ordered according to the degree of symmetry of anion: [Emim]$_2$[PtCl_4] (Entry 18, D_{4h})[19] has a far higher meting point (501 K) than that of [Emim]$_2$[CoCl_4] (374 K, Entry 16, T_d) and [Emim]$_2$[NiCl_4] (365 K, Entry 17, T_d).[17] The influence of the symmetry of the anions can also be found in two 1,3-dimethylimidazolium ionic liquids (Entry 19[60] and 20[61]). Increasing the symmetry of anions might result in close packing of the ions and an increase in the melting points. As to anions with the O_h symmetry, six halogen atoms are included in each anion. The number of halogen atoms as well as the high symmetry also result in a stronger interaction and hence a higher melting point. It should be noted that the influence of the symmetry of anions can only be understood for the same cations, anions with similar charges, and same molar ratio of cation to anion.
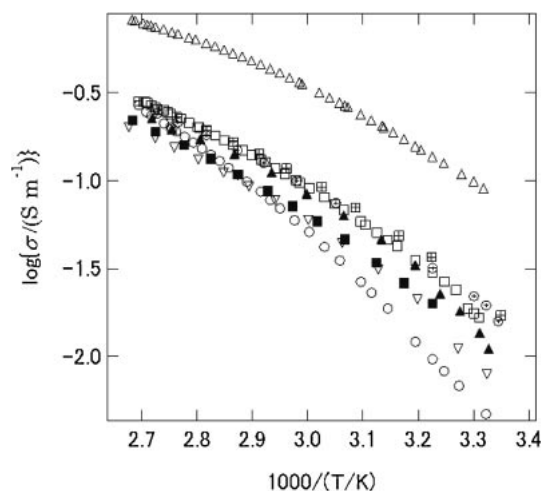

Fig. 3. Arrhenius plots of ionic conductivities. Symbols for [Bmim]$_2$[MCl_4] (M = Sn (**2**, triangles); Cu (**3**, squares); Ni (**4**, filled squares); Mn (**5**, squares with cross); Fe (**6**, circles with cross); Co (**7**, filled triangles); Zn (**8**, down-pointing triangles), and [Bmim]Cl (**1**, circles).

However, exceptions cannot be excluded in the cases of large difference in mass of anions, markedly different crystal structures, and different hydrogen-bonding strength.

Ionic Conductivity. In order to investigate the ionic mobility, the temperature dependence of ionic conductivities of the nine salts were measured in the temperature range from room temperature to 373 K. The Arrhenius plots of ionic conductivity are shown in Fig. 3. Measurements of ionic liquids, which are solids at room temperature, were started from supercooled states under nitrogen atmosphere. At the same temperature, **3**–**8** have similar values of conductivity, which may be due to the similar structures and sizes of their anions. It is notable that **2** showed ionic conductivity about 3 times larger than those of **3**–**8**. The Arrhenius plots of ionic conductivity of homogeneous electrolytes usually exhibit straight or curved relationship. Figure 3 shows that the data points in the Arrhenius plot follow a curve rather than a straight line, indicating non-Arrhenius behavior, which is alternatively treated by the empirical VTF (Vogel–Tammann–Fulcher) equation (Eq. 1) taking viscosity into consideration.[62–64]

$$\sigma = \sigma_0 T^{-1/2} \exp[-B/k(T - T_0)]. \tag{1}$$

To treat the data quantitatively, fitting of the data points by the following modified VTF equation (Eq. 2) was performed:

$$\ln(\sigma T^{1/2}) = \ln A - E_a'/(T - T_0), \tag{2}$$

where T_0 is the glass transition temperature, E_a' is a constant called pseudo-activation energy and represents the energy necessary for creating enough free volume for ion movement, and parameter A relates to the number of charge carriers. An electrolyte with a low E_a' and large $\ln A$ has a higher ionic conductivity. The plot of $\ln(\sigma T^{1/2})$ versus $1/(T - T_0)$ is a straight line, and parameters $\ln A$ and E_a' can be obtained from the y-intercept and the slope, respectively. Although T_0 is usually determined experimentally, here, it was determined by changing T_0 gradually so that the value of R^2 of the fitting straight line is closest to 1. The fitted lines and the obtained values
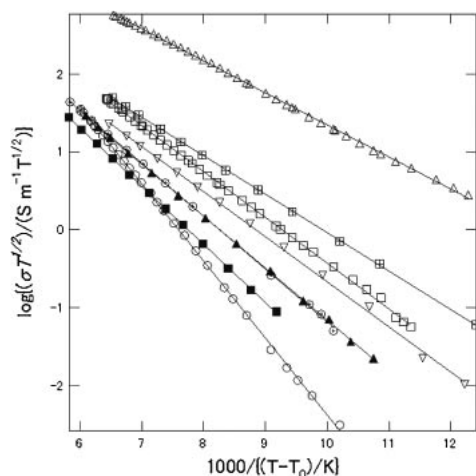
Fig. 4.   The best-fit VTF plots for [Bmim]$_2$[MCl$_4$] (M = Sn (**2**, triangles); Cu (**3**, squares); Ni (**4**, filled squares); Mn (**5**, squares with cross); Fe (**6**, circles with cross); Co (**7**, filled triangles); Zn (**8**, down-pointing triangles), and [Bmim]Cl (**1**, circles). The full lines are the fitting equations.
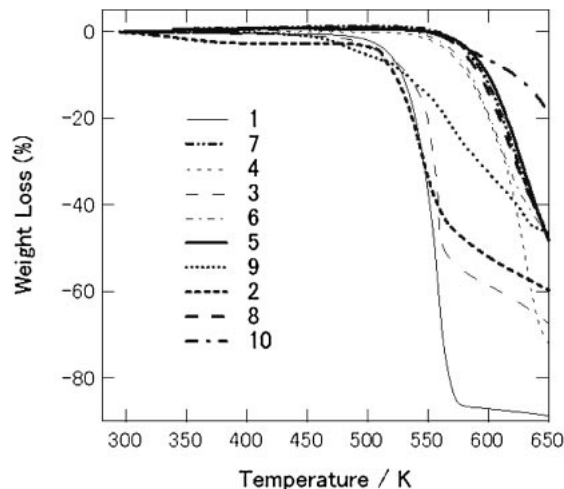

Fig. 5.   Thermal gravimetric analysis of [Bmim]$_2$[MCl$_4$] (M = Sn (**2**), Cu (**3**), Ni (**4**), Mn (**5**), Fe (**6**), Co (**7**), Zn (**8**), and Pt (**9**)), [Bmim]$_2$[ZrCl$_6$] (**10**), and [Bmim]Cl (**1**).

Table 4.   Fitting Parameters Obtained from the VTF Equation, the Conductivities (σ) and the Molar Conductivities (Λ) at 300 K for Ionic Liquids

ILs	T_0/K	E_a'/K	$\ln A$/K$^{1/2}$ S m^{-1}	R^2	σ/10^{-3} S m^{-1}	Λ/10^{-6} S m^2 mol^{-1}
[Bmim]Cl(**1**)	203	989	7.51	0.9996	3.94	0.59
[Bmim]$_2$[SnCl$_4$](**2**)	220	412	5.46	0.9995	78.7	27.4
[Bmim]$_2$[CuCl$_4$](**3**)	214	588	5.45	0.9996	14.4	4.87
[Bmim]$_2$[NiCl$_4$](**4**)	201	747	5.79	0.9999	9.98	3.48
[Bmim]$_2$[MnCl$_4$](**5**)	218	494	4.90	0.9999	18.7	6.67
[Bmim]$_2$[FeCl$_4$](**6**)	200	679	5.61	0.9999	17.7	6.25
[Bmim]$_2$[CoCl$_4$](**7**)	209	668	5.52	0.9998	9.35	3.27
[Bmim]$_2$[ZnCl$_4$](**8**)	218	579	5.12	0.9987	8.29	2.90

of $\ln A$ and E_a' are shown in Fig. 4 and Table 4, respectively. Similar treatment was adopted for ionic liquids prepared by the neutralization of alkylimidazole and inorganic acids measured by either DSC or calculated value through fitting into the VTF equation for ionic conductivity.[25]

All of the values of R^2 of the fitted lines (Table 4) are larger than 0.998, which shows that the experimental data can be fitted to the VTF equation, as seen in Fig. 4. It can be seen in Table 4 that all of the ionic liquids show similar T_0 values at ca. 200 K. Salt **2** shows the highest ionic conductivity, and salts **1** and **3**–**8** show almost similar behavior. From the VTF analysis, salt **2** had the lowest E_a' (412 K), indicating that the energy barrier for ionic mobility is smallest in agreement with the lowest melting point. The effect of large value of A for **1** on conductivity is counteracted by its large E_a' (989 K) among these ionic liquids, which lowers its mobility. From the results of the X-ray crystal structure analysis, it is easy to estimate the total ion density using D_{calcd} values, assuming that the density of the super-cooled states is almost the same as that of the crystal phase. Total ion density for salts **2**–**8** lies in the range 8.3–8.9×10^{-3} mol cm^{-3}, while for the salt **1** it is estimated to be 13.4–13.9×10^{-3} mol cm^{-3} using the reported D_{calcd} values for [Bmim]Cl crystal phases.[20,21] Obtained $\ln A$ values in Table 4 appeared in a rather narrow range 4.90–

5.79 for the salts **2**–**8** except that for the salt **1** (7.51), showing that it is possible to estimate the total ion density based on D_{calcd} values.

The molar conductivity can be estimated using the estimated density values. The conductivity and the molar conductivity at 300 K for each salt are also included in Table 4. It is clear that the Sn salt exhibits the highest molar conductivity, and the salts with T_d local symmetry show similar values. [Bmim]Cl has the lowest molar conductivity. It is obvious that the content of water has no relation on the results of conductivity.

Thermal Stability and Vapor Pressure.   The thermal stability of **1**–**10** were evaluated by thermal gravimetric analysis (TGA), as shown in Fig. 5. Decomposition temperatures (shown in Table 3) were estimated using temperatures at 1% weight losses. Salt **2** exhibited a slight weight loss at 320–370 K, which may be ascribed to the desorption of water. By comparing with the decomposition temperature of salt **1**, the decomposition temperatures fall into three groups: about 20 K lower than **1** (**3** and **9**), about 25 K higher than **1** (**2**), and about 75 K higher than **1** (**4**–**8** and **10**). Because all 10 salts contain the same cation, the difference in the decomposition temperatures is ascribed to the difference in the anions. It is known that ionic liquids with nucleophilic anions (e.g., halides) decompose at lower temperatures than those with
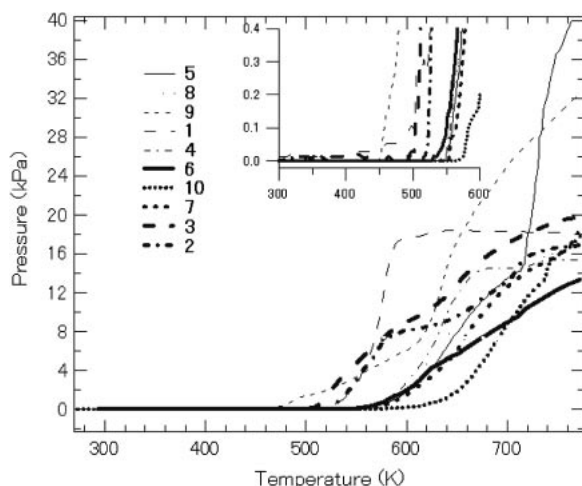
Fig. 6. Vapor pressures of ionic liquids [Bmim]$_2$[MCl$_4$] (M = Sn (**2**), Cu (**3**), Ni (**4**), Mn (**5**), Fe (**6**), Co (**7**), Zn (**8**), and Pt (**9**)), [Bmim]$_2$[ZrCl$_6$] (**10**), and [Bmim]Cl (**1**) in vacuum.

bulky fluorinated anions (low nucleophilicity),[56,59] and S$_N$2 attack of nucleophiles on alkyl groups has been proposed to explain this phenomenon.[65] The catalytic effect of metal ions present in the anions affects the stability of ionic liquids and makes the decomposition pattern complicated.[54] It is well known that stable metal carbene complexes can be synthesized from imidazolium salts and metal compounds in the presence of bases.[66]

The vapor pressures of the ionic liquids were also measured in a vacuum system, and the results are shown in Fig. 6. The onset of the pressure rise for each ionic liquid coincided with that of the weight loss in TGA. For **4–8** and **10**, the vapor pressures were below the detection limit ($\approx$13 Pa) before decomposition. Thermal stability and negligible vapour pressure suggest that the synthesized ionic liquid salts can be used in a variety of applications such as gas/liquid catalytic system and thin films prepared under vacuum condition for surface science studies.

Conclusion

A series of tetra- or hexa-chlorometalate ion-containing ionic liquids [Bmim]$_2$[MCl$_4$] (M = Sn (**2**), Cu (**3**), Ni (**4**), Mn (**5**), Fe (**6**), Co (**7**), Zn (**8**), and Pt (**9**)) and [Bmim]$_2$[ZrCl$_6$] (**10**) were synthesized, and their crystal structures were determined by X-ray crystal structure analysis. To the best of our knowledge, **2**, **5**, **6**, and **8** are the first ionic liquids containing Sn^{2+}, Mn^{2+}, Fe^{2+}, and Zn^{2+} ions, respectively, to be crystallographically characterized. The ionic liquid character of the nine salts was confirmed by the measurements of melting point, ionic conductivity, TGA, and vapor pressure. **2** and **3** are room temperature ionic liquids with the relatively low melting points of 278 and 296 K, respectively, due to the low symmetry of the anions. The melting points of the present salts can be closely correlated to the symmetry of anions. Interactions between [Bmim]$^+$ and anions through C–H$\cdots$Cl hydrogen bonding were found. The imidazolium cation ring edge is directed to anion to maximize the formation of hydrogen bonds. The interactions between the cations through C–

H$\cdots\pi$ and/or $\pi\cdots\pi$ interactions were also found. The effects of hydrogen bonding on the crystal structures were discussed. The ionic conductivity in the super-cooled state as a function of temperature was successfully interpreted with the VTF equation using parameters based on the crystallographic results. The synthesized salts had high thermal stability and negligible vapor pressure below their decomposition temperatures.

Supporting Information

Elemental analysis, NMR assignments, and detailed crystal structural interpretations. This material is available free of charge on the web at http://www.csj.jp/journals/bcsj/.

References

1   C. L. Hussey, *Pure Appl. Chem.* **1988**, *60*, 1763.
2   T. Welton, *Chem. Rev.* **1999**, *99*, 2071.
3   P. Wasserscheid, W. Keim, *Angew. Chem.* **2000**, *39*, 3772.
4   R. Hagiwara, Y. Ito, *J. Fluorine Chem.* **2000**, *105*, 221.
5   J. Dupont, R. F. de Souza, P. A. Z. Suarez, *Chem. Rev.* **2002**, *102*, 3667.
6   C. M. Gordon, *Appl. Catal., A* **2001**, *222*, 101.
7   H. Olivier-Bourbigou, L. Magna, *J. Mol. Catal. A: Chem.* **2002**, *182–183*, 419.
8   J. E. L. Dullius, P. A. Z. Suarez, S. Einloft, R. F. de Souza, J. Dupont, *Organometallics* **1998**, *17*, 815.
9   D. Zhao, Z. Fei, T. J. Geldbach, R. Scopelliti, P. J. Dyson, *J. Am. Chem. Soc.* **2004**, *126*, 15876.
10   T. Sasaki, C. Zhong, M. Tada, Y. Iwasawa, *Chem. Commun.* **2005**, 2506.
11   K. R. Seddon, *J. Chem. Technol. Biotechnol.* **1997**, *68*, 351.
12   T. B. Scheffler, M. S. Thomson, Seventh International Conference on Molten Salts, Montreal, Canada, **1990**, p. 281.
13   A. P. Abbott, G. Capper, D. L. Davies, H. L. Munro, R. K. Rasheed, V. Tambyrajah, *Chem. Commun.* **2001**, 2010.
14   A. P. Abbott, G. Capper, D. L. Davies, R. Rasheed, *Inorg. Chem.* **2004**, *43*, 3447.
15   R. J. C. Brown, P. J. Dyson, D. J. Ellis, T. Welton, *Chem. Commun.*, **2001**, 1862.
16   P. B. Hitchcock, R. J. Lewis, T. Welton, *Polyhedron* **1993**, *12*, 2039.
17   P. B. Hitchcock, K. R. Seddon, T. Welton, *J. Chem. Soc., Dalton Trans.* **1993**, 2639.
18   M. Hasan, I. V. Kozhevnikov, M. R. H. Siddiqui, A. Steiner, N. Winterton, *Inorg. Chem.* **1999**, *38*, 5637.
19   M. Hasan, I. V. Kozhevnikov, M. R. H. Siddiqui, C. Femoni, A. Steiner, N. Winterton, *Inorg. Chem.* **2001**, *40*, 795.
20   S. Saha, S. Hayashi, A. Kobayashi, H. Hamaguchi, *Chem. Lett.* **2003**, *32*, 740.
21   J. D. Holbrey, W. M. Reichert, M. Nieuwenhuyzen, S. Johnston, K. R. Seddon, R. D. Rogers, *Chem. Commun.* **2003**, 1636.
22   A. Elaiwi, P. B. Hitchcock, K. R. Seddon, N. Srinivasan, Y.-M. Tan, T. Welton, J. A. Zora, *J. Chem. Soc., Dalton Trans.* **1995**, 3467.

23 P. Kölle, R. Dronskowski, *Inorg. Chem.* **2004**, *43*, 2803.

24 Y. Yoshida, K. Muroi, A. Otsuka, G. Saito, M. Takahashi, T. Yoko, *Inorg. Chem.* **2004**, *43*, 1458.

25 H. Ohno, M. Yoshizawa, *Solid State Ionics* **2002**, *154–155*, 303.

26 H. Matsumoto, T. Matsuda, Y. Miyazaki, *Chem. Lett.* **2000**, 1430.

27 T. Nishida, Y. Tashiro, M. Yamamoto, *J. Fluorine Chem.* **2003**, *120*, 135.

28 K. Matsumoto, R. Hagiwara, Y. Ito, *J. Fluorine Chem.* **2002**, *115*, 133.

29 Y. Katayama, I. Konishiike, T. Miura, T. Kishi, *J. Power Sources* **2002**, *109*, 327.

30 W. Xu, E. I. Copper, C. A. Angell, *J. Phys. Chem. B* **2003**, *107*, 6170.

31 S. A. Bolkan, J. T. Yoke, *J. Chem. Eng. Data* **1986**, *31*, 194.

32 G. Saito, in *Ionic Liquids: The Front and Future of Material Development*, ed. by H. Ohno, **2003**.

33 S. Hayashi, H. Hamaguchi, *Chem. Lett.* **2004**, *33*, 1590.

34 M. S. Sitze, E. R. Schreiter, E. V. Patterson, R. G. Freeman, *Inorg. Chem.* **2001**, *40*, 2298.

35 C. Zhong, T. Sasaki, M. Tada, Y. Iwasawa, *J. Catal.* **2006**, *242*, 357.

36 A. Altomare, M. C. Burla, M. Camalli, G. Cascarano, C. Giacovazzo, A. Guagliadi, G. Polidori, *J. Appl. Crystallogr.* **1994**, *27*, 435.

37 M. N. Burnett, C. K. Johnson, *ORTEP-III: Oak Ridge Thermal Ellipsoid Plot Program for Crystal Structure Illustrations*, Oak Ridge National Laboratory Report, **1996**.

38 D. Reinen, M. Atanasov, G. S. Nikolov, F. Steffens, *Inorg. Chem.* **1988**, *27*, 1678.

39 D. W. Smith, *Coord. Chem. Rev.* **1976**, *21*, 93.

40 K. E. Halvorson, C. Patterson, R. D. Willett, *Acta Crystallogr., Sect. B* **1990**, *46*, 508.

41 P. G. Harrison, in *Silicon, Germanium, Tin and Lead*, ed. by G. Wiikinson, **1987**.

42 J. K. Stalick, P. W. R. Corfield, D. W. Meek, *Inorg. Chem.* **1973**, *12*, 1668.

43 H. J. Haupt, F. Huber, H. Preut, *Z. Anorg. Allg. Chem.* **1976**, *422*, 97.

44 L. J. W. Shimon, M. Vaida, L. Addadi, M. Lahav, L. Leiserowitz, *J. Am. Chem. Soc.* **1990**, *112*, 6215.

45 E. M. D. Keegstra, A. L. Spek, J. W. Zwikker, L. W. Jenneskens, *J. Chem. Soc., Chem. Commun.* **1994**, 1633.

46 G. R. Desiraju, *Angew. Chem., Int. Ed. Engl.* **1995**, *34*, 2311.

47 G. R. Desiraju, *Acc. Chem. Res.* **2002**, *35*, 565.

48 R. Taylor, O. Kennard, *J. Am. Chem. Soc.* **1982**, *104*, 5063.

49 C. B. Aakeroy, T. A. Evans, K. R. Seddon, I. Palinko, *New J. Chem.* **1999**, *23*, 145.

50 A. Bondi, *J. Phys. Chem.* **1964**, *68*, 441.

51 R. Ozawa, S. Hayashi, S. Saha, A. Kobayashi, H. Hamaguchi, *Chem. Lett.* **2003**, *32*, 948.

52 G. Ling, N. Koura, *Denki Kagaku* **1997**, *65*, 149.

53 L. P. Battaglia, A. B. Corradi, G. Marcotrigiano, L. Menabue, G. C. Pellacani, *Inorg. Chem.* **1982**, *21*, 3919.

54 C. K. Lee, H. H. Peng, I. J. B. Lin, *Chem. Mater.* **2004**, *16*, 530.

55 J. D. Holbrey, K. R. Seddon, *J. Chem. Soc., Dalton Trans.* **1999**, 2133.

56 H. L. Ngo, K. LeCompte, L. Hargens, A. B. McEwen, *Thermochim. Acta* **2000**, *357–358*, 97.

57 J. G. Huddleston, A. E. Visser, W. Matthew, H. D. Willauer, G. A. Brocker, R. D. Rogers, *Green Chem.* **2001**, *3*, 156.

58 H. Stegemann, A. Rhode, A. Reiche, A. Schnittke, H. Fullbier, *Electrochim. Acta* **1992**, *37*, 379.

59 D. M. Fox, W. H. Awad, J. W. Gilman, P. H. Maupin, H. C. DeLong, P. C. Truove, *Green Chem.* **2003**, *5*, 724.

60 J. D. Holbrey, W. M. Reichert, R. P. Swatloski, G. A. Brocker, W. R. Pitner, K. R. Seddon, R. D. Rogers, *Green Chem.* **2002**, *4*, 407.

61 S. V. Dzyuba, R. A. Bartsch, *Chem. Commun.* **2001**, 1466.

62 H. Vogel, *Phys. Z.* **1921**, *22*, 645.

63 G. Tammann, W. Hesse, *Z. Anorg. Allg. Chem.* **1926**, *156*, 245.

64 G. S. Fulcher, *J. Am. Ceram. Soc.* **1925**, *8*, 839.

65 A. G. Glenn, P. B. Jones, *Tetrahedron Lett.* **2004**, *45*, 6967.

66 D. Bourissou, O. Guerret, F. P. Gabbai, G. Bertrand, *Chem. Rev.* **2000**, *100*, 39.